Iris Color and Texture: A Comparative Analysis of Real Irises, Ocular Prostheses, and Colored Contact Lenses

Jorge A. Herrera,[1] Meritxell Vilaseca,[1]* Jochen Düll,[2] Montserrat Arjona,[1] Elena Torrecilla,[3] Jaume Pujol[1]

[1]Centre for Sensors, Instruments and Systems Development (CD6), Department of Optics and Optometry, Universitat Politècnica de Catalunya, Terrassa, Barcelona, Spain

[2]Fachbereich Mathematik und Naturwiss en schaften, University of Applied Sciences, Darmstadt, Germany

[3]Marine Technology Unit (UTM, CSIC), Consejo Superior de Investigaciones Científicas, Barcelona, Spain

Received 17 December 2009; revised 29 March 2010; accepted 1 April 2010

*Abstract: In this work, we analyzed the color and texture of irises, ocular prostheses, and cosmetic colored contact lenses measured by means of a multispectral system, which provides the CIE L*a*b* colorimetric coordinates of a high resolution image pixel by pixel. The same subject, who has dark brown irises, participated in the measurement of all the contact lenses. The CIE L*a*b* colorimetric coordinates were analyzed to classify the samples into three major groups (brown, blue and green) using a new algorithm developed for this purpose. This classification allowed us to carry out a comparison of the color associated with each set of samples, using the corresponding color gamuts in the CIE L*a*b* color space. Furthermore, we analyzed the iris color reproduction achieved by prostheses and contact lenses in terms of CIEDE2000 color differences, and obtained closer results with prostheses. In addition, we performed an analysis of texture by means of the color spatial distribution of all samples. This was achieved by means of two statistical approaches: first order statistics of image histograms and second order statistics using co-occurrence matrices. The results suggest that the texture associated with real irises, ocular prostheses and colored contact lenses is very different. This study provides useful information about the color and texture of irises that may help to establish a strategy for improving the techniques used in the manufacturing process of prostheses and colored contact lenses to obtain a better and more realistic appearance.* © 2010 Wiley Periodicals, Inc. Col Res Appl, 00, 000–000, 2010; Published online in Wiley Online Library (wileyonlinelibrary.com). DOI 10.1002/col.20635

Key words: color measurement; multispectral systems; texture; iris; CIEDE2000 color difference

INTRODUCTION

The study of the human iris is of interest because of the wide range of areas in which it plays a role, such as aesthetics, health and biometrics. In several articles, relationships have been established between the color of irises and various physiological conditions.[1–3] In addition, color is the key to the relatively recent use of irises as a biometric tool, in which their specific texture is also taken into account,[4–6] although one must have in mind that final appearance of human irises depends on other factors such as the color of the skin.

Traditionally, the measurement of the color of irises in areas in which this is an important issue has been performed by means of subjective assessments. An example can be found in ocular prostheses manufacturing, in which trained observers classify irises into discrete color groups.[7–9] More recent studies have included new tools based on conventional colorimetric devices[2,10–13] or even digital imaging systems[12,13] to acquire and process data by looking for objective and quantitative measurements. The advantages of these tools are as follows: better accu-

*Correspondence to: Meritxell Vilaseca (e-mail: mvilasec@oo.upc.edu).

Contract grant sponsor: Spanish Ministry of Science and Innovation; contract grant number: DPI2008-06455-C02-01.

racy in grading samples, increased repeatability, lower processing time as analyses are automatic, and better data access for statistical and mathematical analyses.

However, most of the color characterizations of irises have been restricted to mean colorimetric measurements, and have not analyzed spatial color distribution, that is, iris texture. Iris texture has mainly been studied in relation to iris recognition systems,[4–6,11,14–16] which use the variability of iris patterns to produce codes that identify each iris unfailingly, since irises have a probability of 1 in 10^{78} of being the same.[4] In such applications, color information is not as important as it is in other cases. In fact, iris texture analysis in recognition systems is typically performed by imaging near infrared light.[16] As Melgosa *et al.*[10] showed with a systematic comparison between objective and subjective color assessments for real and prosthetic iris color matching, overall color values are not enough for a complete characterization of the iris. Hence, information on spatial colorimetric features or color texture can be useful in some specific applications, such as ocular prosthesis or colored contact lens manufacturing,[17,18] in which color and texture reproduction is of great importance. In this context, some attempts have been done to develop methods for modelling and rendering the structure of human irises to obtain a more realistic appearance,[19,20] although their use in this field is still limited.

The use of multispectral imaging technology,[11,21–23] which commonly employs high resolution optoelectronic sensors to acquire the scene through several spectral bands, provides the opportunity to acquire high spatial resolution images with access to color and spectral data pixel by pixel. In this study, we carried out color and texture analyses of three sets of samples analyzed by means of a multispectral system developed in a former article:[23] real irises, ocular prostheses, and cosmetic colored contact lenses.

This article is structured as follows: In the following section, we describe the samples and the experimental setup of the multispectral system used to compute the CIE $L^*a^*b^*$ color coordinates. In the "Method" section, we present the colorimetric and textural tools used to describe the samples. In the "Results and Discussion" section, we show the color comparison of samples by means of gamuts in the CIE $L^*a^*b^*$ color space as well as the CIEDE2000 color differences. Furthermore, we report on the differences found among samples in terms of texture. The last section contains the most relevant "Conclusions."

EXPERIMENTAL SETUP AND SAMPLES

The multispectral system[23] used to obtain magnified images of the entire irises, ocular prostheses, and colored contact lenses was a 12-bit depth cooled CCD monochrome camera (QImaging QICAM Fast1394 12 bit) with 1.4 MPixels (1392 × 1040), an objective zoom lens (Nikon AF Nikkor 28–105 mm), and an RGB tunable filter. The system was also composed of a halogen lamp (Philips 15V 150W) attached to a stabilized DC power supply and a focusing lens. This allowed the analyzed samples to be lit with a 45° angle of incidence (Fig. 1). A flat field correction was applied to the acquired images, to correct the camera response and the nonuniformity of the illumination.[24] The system allowed the reconstruction of spectral reflectance profiles pixel by pixel using Moore-Penrose pseudoinverse-based algorithms.[25,26] To simplify the color comparison among samples, the CIE $L^*a^*b^*$ colorimetric coordinates were obtained under the daylight illuminant D65 and the CIE-1931 standard observer from the computed spectra. Therefore, three colorimetric images in terms of CIE $L^*a^*b^*$ coordinates were available for each sample. The system also incorporated a telespectra-colorimeter (Photo Research PR-655 with the accessory MS-75), which enabled the performance of the system to be checked at any time.

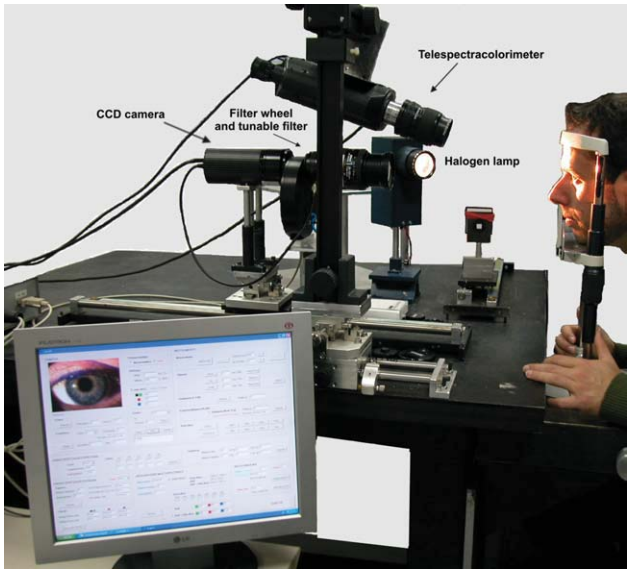

FIG. 1. Multispectral system (experimental setup).

The samples were 106 real human irises from 53 Spanish individuals, in which irises containing the color brown are the most common; 68 ocular prostheses provided by Ovidio S.L. (Barcelona, Spain) and used in daily clinical practice; and 17 colored contact lenses (CIBA VISION Fresh Look) corresponding to all of the colorations provided by the manufacturer. The same subject, who has dark brown irises, participated in the measurement of all the contact lenses.

As an example, Fig. 2 shows the reconstructed spectral reflectance profiles from the images acquired by the multispectral system of three blue samples, as well as their corresponding CIE $L^*a^*b^*$ coordinates.

METHOD

Analysis of Color

To perform the color comparison among the irises, ocular prostheses, and colored contact lenses, we analyzed the averaged CIE $L^*a^*b^*$ coordinates that corresponded to two square areas of $\sim$1 mm^2 on samples with a rather

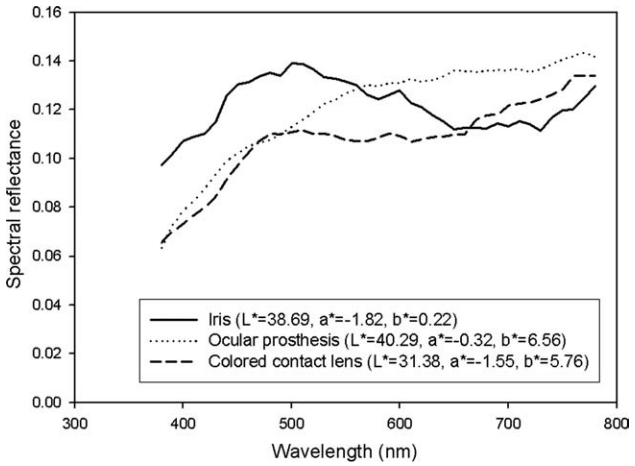

FIG. 2. Reconstructed spectral reflectances of three blue samples (iris, ocular prosthesis, and colored contact lens) and the corresponding CIE *L*a*b** coordinates.

uniform coloration (Fig. 3). As shown in the figure, these areas corresponded to zones with the predominant coloration of the eye. Parts of the iris with a clearly different color were avoided.

To make the color comparison among samples much easier, an automatic algorithm was developed to classify them into three color groups: brown, blue, and green. This algorithm established borders in the CIE *L*a*b** space using an optimization procedure based on a preliminary subjective visual classification, to define a volume for each color group, by means of specific criteria from the analysis of the *L**, *a**, *b**, C^*_{ab} (chroma) and $h_{ab}(^\circ)$ (hue-angle) coordinates of the samples, and the application of some logical conditions (AND and OR operators) to them (Table I). In the preliminary visual classification, a trained examiner analyzed the color of each iris, ocular prosthesis, and colored contact lens under the influence of a D65 daylight simulator, and classified them accordingly to his subjective observations.

This classification allowed us to visualize the color gamut corresponding to the brown, blue, and green groups of the real irises, ocular prostheses and colored contact lenses respectively, and to compare them over a 3D representation in the CIE *L*a*b** color space.

To study the color reproduction achieved by ocular prostheses and colored contact lenses compared to real irises, we calculated the CIEDE2000 color differences.[27] In this context, we looked for the closest pair to each real iris in the other two sample sets (ocular prostheses and colored contact lenses), in terms of the CIEDE2000 color difference.

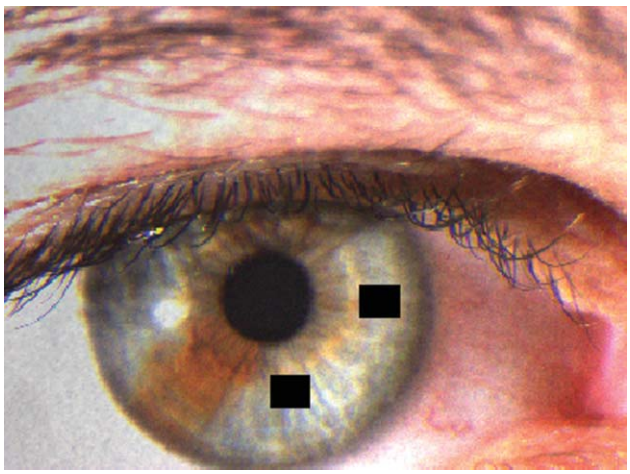

FIG. 3. Iris sample showing the areas from which the mean colorimetric values are extracted.

TABLE I. L*, a*, b*, C^*_{ab} and $h_{ab}(^\circ)$ coordinates used for the establishment of borders in the CIE L*a*b* space.

	LOG1										
	LOG1.1				LOG1.2			LOG2			LOG3
Brown											
L*		OR		NOT	>27	OR		OR	<26	OR	<26
a*	>7		>7		>7		>7				<7
b*			>0		>0						>0
C^*_{ab}					≤11				<11		
$h_{ab}(^\circ)$	>338						>338				
Blue	LOG1					OR	LOG2	OR		LOG3	
L*	>26									>26	
a*							<0				
b*							<0				
C^*_{ab}	≤11						>11				
$h_{ab}(^\circ)$									<270 AND >338		
Green	LOG1										
L*	>27										
a*	<7										
b*	>0										
C^*_{ab}	>11										
$h_{ab}(^\circ)$	>270 AND <338										

LOG refers to logical conditions that samples must satisfy to be classified into one of the three color groups: brown, blue, and green. An AND operator is applied to cells corresponding to the same column, meanwhile and OR operator is applied between complete columns. In the case of the brown group, there is also a NOT operator, meaning that samples can be classified as brown if condition LOG1.1 is verified and LOG1.2 is not, or vice versa.

Analysis of Texture

In addition to the former mean colorimetric evaluation, we analyzed the spatial color distribution, or equivalently the texture, over the analyzed samples, since the multispectral system that we used enabled us to obtain spectral information on the samples pixel by pixel.

For this purpose, we first developed a complete set of segmentation algorithms to extract the iris region from the entire image of the eye acquired by the multispectral system. These algorithms involved a first step of pupil detection, which consisted of a variable thresholding procedure followed by a blob analysis for measuring the region properties of eccentricity and solidity,[28] which is suitable for identifying round-like shapes. Then, the iris border was determined by means of a Kirsch edge enhancement filter followed by an ellipse shape search using Hough transform.[29] This ellipsoidal border of the iris, specifically the upper half of it, was then used to track two points for drawing a line where the eyelid was present. Finally, the specular reflection of the illumination system that was present in the image was removed with a similar procedure to that implemented in the pupillary border determination. This process allowed proper separation of the iris region from the other parts of the image (Fig. 4). Thus, only the pixels belonging to the iris region were taken into account in further analyses.

Once the images had been segmented, a textural analysis of the samples could be performed. To simplify this, the three-channel CIE $L^*a^*b^*$ images were replaced by a one-channel CIEDE2000 color difference image, which also provided good computational performance. This image was computed as the CIEDE2000 color difference between every pixel and the mean CIE $L^*a^*b^*$ coordinates of the entire sample. This preprocessing procedure highlighted structures that deviated from the mean color.

As a first approach to the extraction of texture information, we used the study of statistical properties of the image histogram, also known as first order statistics.[28] This analysis included the study of some features, such as entropy (Ep), a well known statistical measure of randomness,[28,29] energy (En), numerical descriptor of the image uniformity having 1 as its maximum value for a constant image and, in our case, the third central moment (μ_3), which account for the skewness of the histogram. The mathematical description of these features can be seen in the following equations:

$$Ep = -\sum_{i=0}^{N-1} P_i \log_2(P_i), \tag{1}$$

$$En = \sum_{i=0}^{N-1} P_i^2, \tag{2}$$

$$\mu_3 = \sum_{i=0}^{N-1} (i-m)^3 P_i. \tag{3}$$

where P_i is the value of the element i of the histogram, N is the number of levels that the histogram is divided into and $m = \sum_{i=0}^{N-1} iP_i$ is the mean (average) value.

Likewise, we implemented a second approach based on a co-occurrence matrices[30] algorithm to analyze the color

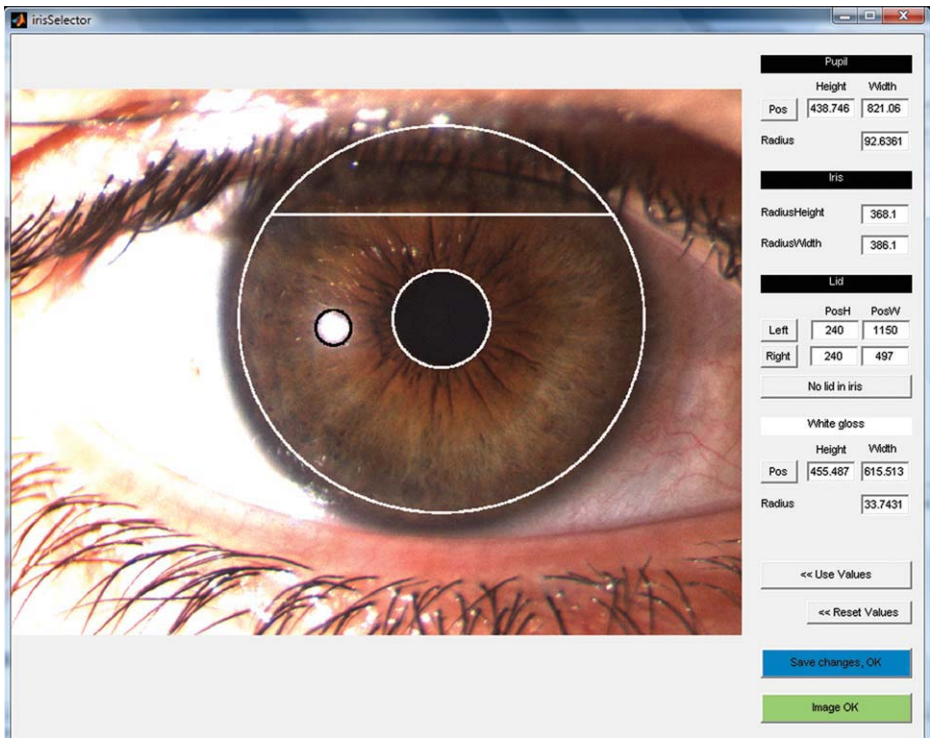

FIG. 4. Screen shot of the application developed in Matlab® for the iris segmentation showing the boundaries that have been found with the algorithm.

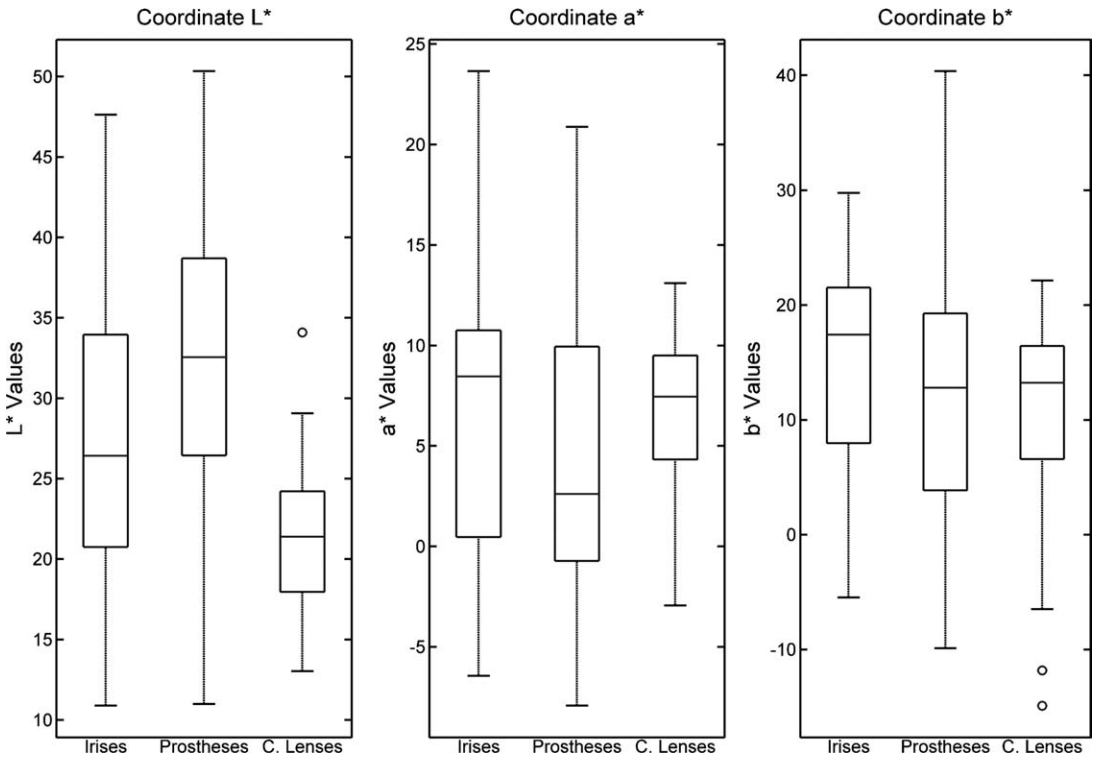

FIG. 5. Box plots showing the distribution of the mean CIE L^* a^* b^* values for real irises, ocular prostheses, and colored contact lenses.

spatial distribution of samples. These matrices can be considered the second order histograms of the image, since they accumulate the occurrence of the levels of two pixels, given an angle and a distance. Thus, they include the spatial relationships between the pixel levels. Co-occurrence matrices can be analyzed through statistical features that are similar to those used formerly (Haralick[30] proposed twelve descriptors for texture analysis). Examples of them are entropy (*Ep*), energy (*En*), and also contrast (*C*), which in this case takes into account the level difference between pixel neighbors:

$$Ep = -\sum_{i,j=0}^{N-1} P_{i,j} \log_2(P_{i,j}), \tag{4}$$

$$En = \sum_{i,j=0}^{N-1} P_{i,j}^2, \tag{5}$$

$$C = \sum_{i,j=0}^{N-1} P_{i,j}(i-j)^2 \tag{6}$$

where $P_{i,j}$ are the values of the element i, j of the co-occurrence matrix.

Statistical texture analysis can be done through first, second or even higher order statistics but, although higher orders are theoretically possible, they are not commonly used due to the better performance, lower computational complexity and easiness of results interpretation with statistics up to second order.[31] Some authors have claimed that human perception is incapable of noticing third or higher order relationships, although there is still an open discussion.[32,33] In our case, second order statistical analysis was enough to find concluding differences among samples. Consequently, higher orders were not considered.

A classification test using texture feature vectors that consisted of the several descriptors as those mentioned before was used to estimate texture differences among the samples. The statistical classifier was based on discriminant analysis[34] with a linear discriminant function, which maximized the ratio of between-class variance to within-class variance, to decide on class membership.

RESULTS AND DISCUSSION

Analysis of Color

Figure 5 uses the box plot tool[35] to visually summarize and compare amongst the groups of samples (real irises, ocular prostheses, and colored contact lenses) the averaged colorimetric data (CIE $L^*a^*b^*$ color coordinates) extracted from the square areas. These plots enable us to observe the distribution of the values, which is shown by means of five statistical descriptors (maximum, 3rd quartile, median, 1st quartile, and minimum), the data symmetry, central tendency and dispersion. The mean CIE $L^*a^*b^*$ color coordinates corresponding to the subject with dark brown irises who participated in the measurement of all the contact lenses were of $L^* = 18.51$, $a^* = 9.77$, and $b^* = 16.28$.

Figure 6 shows the color gamuts in the CIE $L^*a^*b^*$ color space obtained from the automatic classification

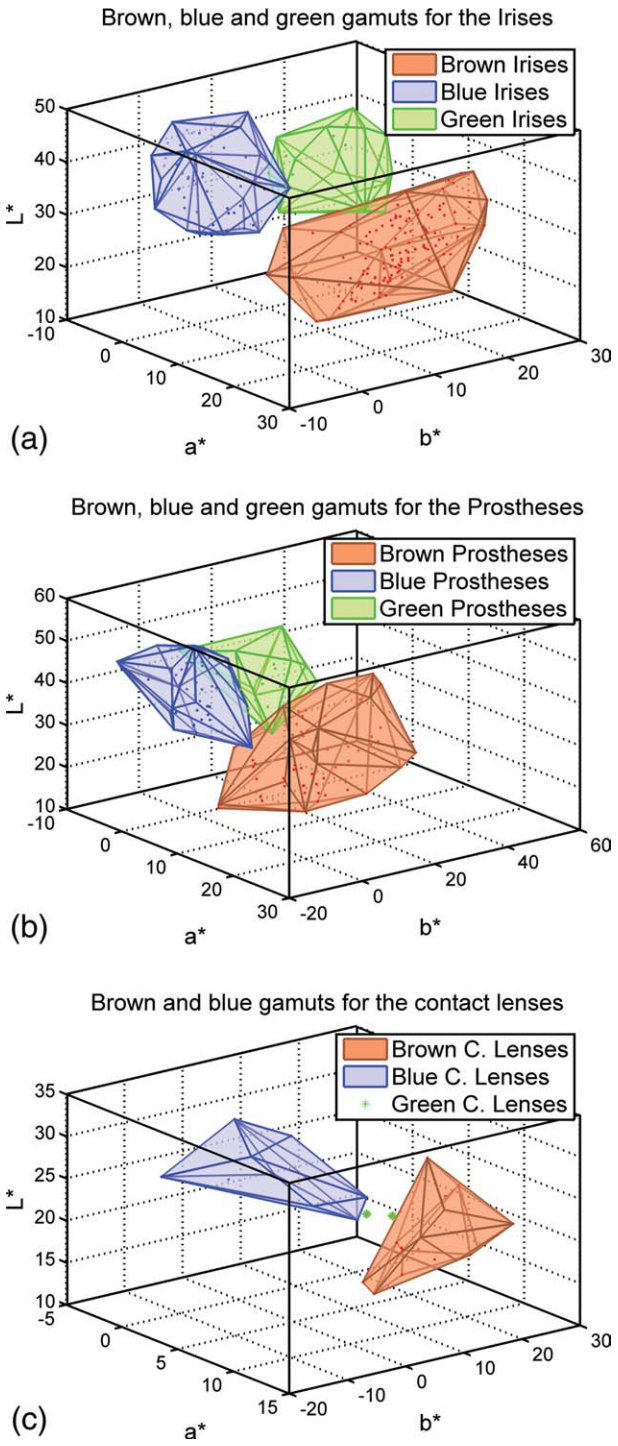

FIG. 6. Classification of square areas in brown, blue and green color groups. (a) Classification for the real irises set, (b) the prostheses set, and (c) the contact lenses set.

applied to the brown, blue, and green color groups. Table II shows the number of square areas corresponding to each color gamut. The results are presented for all samples as well as for irises, prostheses, and contact lenses separately. The volumes shown are the convex hulls[36] for each set of points that arise from the classification. This separation shows that the brown group was the largest and most numerous, both for the whole sample set and

TABLE II. Number of square areas corresponding to brown, blue, and green color groups resulting from the proposed color classification.

	Irises	Prostheses	C. lenses	Total
Brown	130	65	18	213
Blue	59	47	14	120
Green	23	24	2	49
Total	212	136	34	382

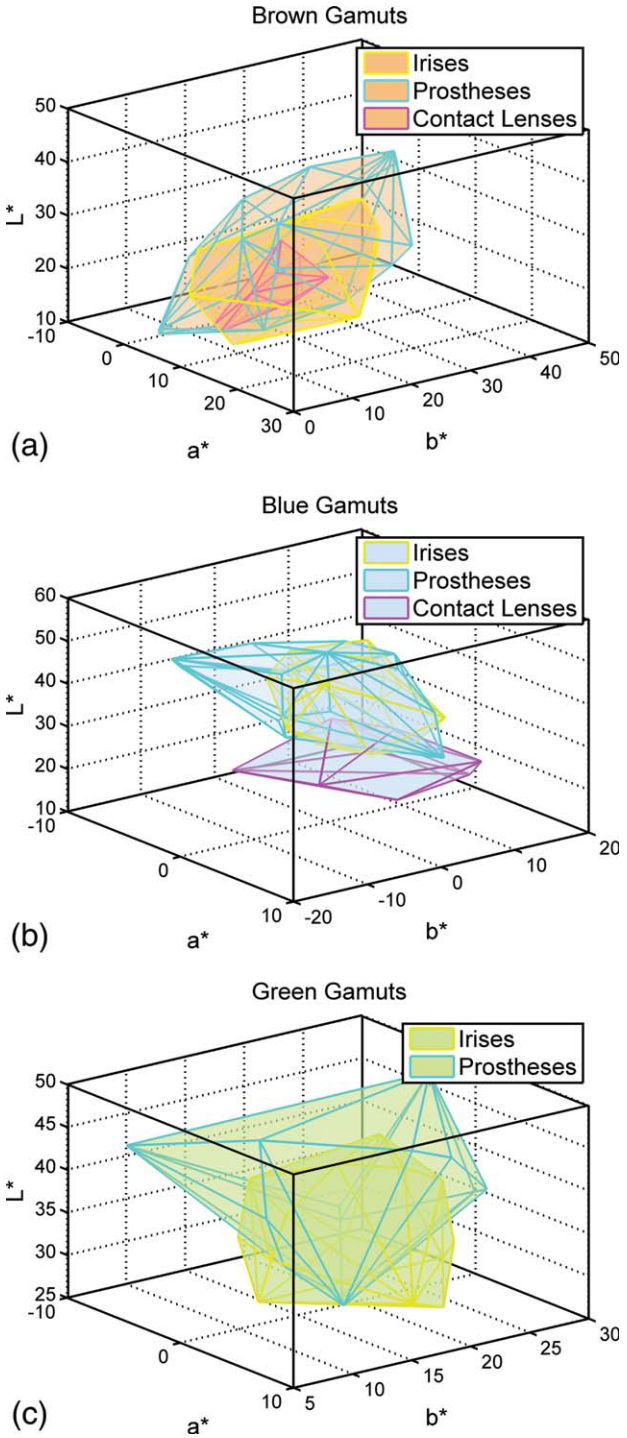

FIG. 7. Gamuts for each color group separated by sample sets. (a) Brown gamuts, (b) blue gamuts, and (c) green gamuts.

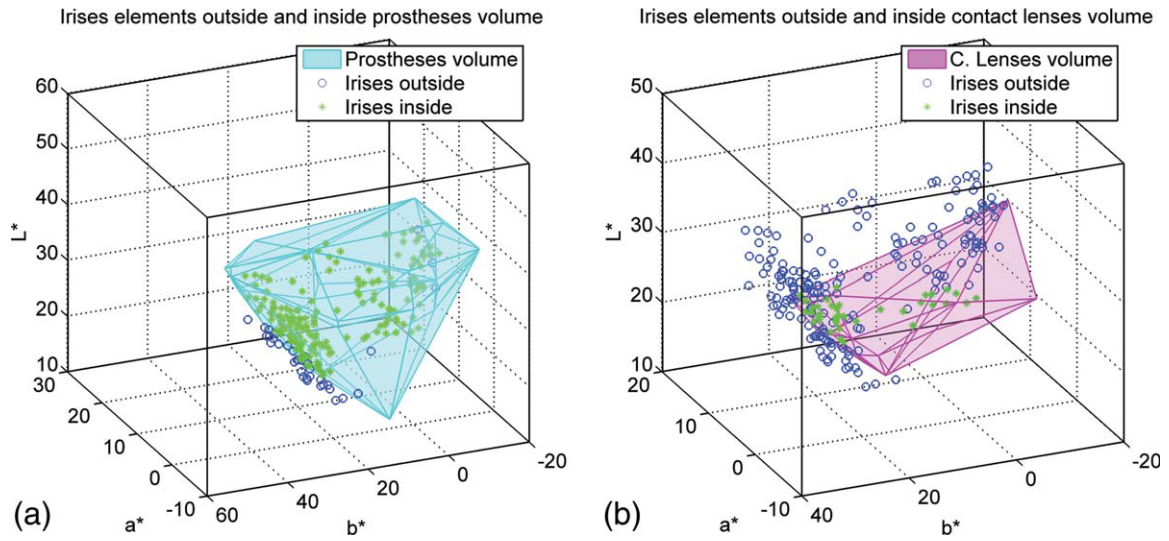

FIG. 8. Elements from the irises group that fall into the prostheses volume (a) and into the contact lenses volume (b) defined by the corresponding gamuts.

for each kind of sample separately. As mentioned earlier, this was expected, because the Spanish population predominantly has brown irises and the subject involved in the contact lens measurements had dark brown irises. In the contact lenses classification, there were not enough elements in the green color group to generate an independent volume. In this case, only two samples were codified as green: two colored contact lenses and the participating subject, who had a dark brown iris.

The former classification allows the comparison of samples by color groups and the qualitative analysis of the iris color reproduction achieved by ocular prostheses and colored contact lenses, taking into account how the gamuts overlap (Fig. 7). This figure shows how the irises and ocular prostheses had a general tendency to be more similar than irises and contact lenses. Specifically, when the brown color groups were analyzed, almost every gamut was contained in the group given by the ocular prostheses. For the blue subsets, ocular prostheses and irises overlapped much more than contact lenses and irises. This behavior was expected, due to the fact that meanwhile ocular prostheses always try to match the color of the iris of the living eye, the colored contact lenses may often try to change the color of the natural irises rather than achieving a good color reproduction. Furthermore, the color gamut associated with contact lenses is very limited. This can be partially explained by the limited number of samples in this set, and the low dispersion of their values in the CIE $L^*a^*b^*$ color space, due to the influence of the brown iris used in the measurement. Finally, for the green samples, the irises and prostheses had a rather similar color gamut, although the overlap was not as large as in the other two color groups considered.

To analyze quantitatively the former observations, Fig. 8 shows the samples from the iris group that fall into the volume defined by the gamuts of ocular prostheses and contact lenses, respectively. Table III supports this figure, and gives the percentages of elements belonging to each iris class that fall into the corresponding volume defined by the gamuts of ocular prostheses and contact lenses. Rather high percentages of superposition are found between irises and ocular prostheses. The comparison between irises and lenses did not provide as good results as expected, even in the case of the brown samples. The percentage could not be given for green contact lenses, since only two elements belonged to this group.

After the gamut comparisons, the color reproduction was evaluated in terms of the CIEDE2000 color difference formula. This was carried out by looking for the ocular prosthesis and contact lens closest to each human iris, that is, with the minimum CIEDE2000 color difference. Table IV shows the mean and the standard deviation of minimum CIEDE2000 color differences when all samples

TABLE III. Percentages of iris samples that fall into the volume defined by the gamuts of ocular prostheses and contact lenses considering all samples and the color groups.

Pair of sets for comparison							
All samples		Brown		Blue		Green	
Irises: prostheses (%)	Irises: C. lenses (%)	Irises: prostheses (%)	Irises: C. lenses (%)	Irises: prostheses (%)	Irises: C. lenses (%)	Irises: prostheses (%)	Irises: C. lenses (%)
82.9	18.0	73.0	18.0	68.0	15.0	56.5	n.a.*

* n.a.: nonapplicable.

TABLE IV. Mean and standard deviation of minimum color CIEDE2000 differences between real irises and ocular prostheses and contact lenses.

	All samples		Brown color		Blue color		Green color	
	Irises: prostheses	Irises: C. lenses	Irises: prostheses	Irises: C. lenses	Irises: prostheses	Irises: C. lenses	irises: prostheses	Irises: C. lenses
Mean	2.36	4.47	2.34	2.42	2.31	8.27	2.51	11.46
Std. Dev.	1.02	3.95	1.15	1.62	0.76	3.87	1.12	4.39

were considered together, as well as with separated color groups. In general, lower color differences were obtained between irises and ocular prostheses than between irises and contact lenses. In the case of prostheses, all color groups provide similar color difference values (similar to or below 2.5 CIEDE2000 units), i.e., similar color reproduction. Higher values were found when irises were compared with contact lenses, which means that, in this case, the reproduction was clearly worse. One exception was observed in the brown color group, in which the results obtained by ocular prostheses and contact lenses were very similar, despite the fact that the lenses and irises had a low superposition percentage. This fact, which appears to be contradictory, may be explained by the small volume associated with brown contact lenses—just a few brown irises fall into that volume. However, the rest of the brown irises still maintained small distances in the CIE $L^*a^*b^*$ color space with respect to the brown contact lenses [Fig. 8(b)].

Finally, the same analysis of color among the considered samples was repeated but taking into account the illuminant A, which is usually more appropriate to simulate indoor environments. The results obtained in terms of color gamuts overlapping and color differences were almost exact to those obtained when using the illuminant D65, and for this reason they are not provided again.

Analysis of Texture

Figure 9 shows the distribution of some of the first order statistical descriptors applied to the texture characterization of samples. The first order statistical descriptors corresponding to the subject with dark brown irises who participated in the measurement of all the contact lenses were of $Ep = 6.83$, $En = 0.011$, and $\mu_3 = 49.67$.

An analysis of the features alone is not sufficient to provide a clear insight into texture, to establish whether this varies among sample classes. Consequently, we constructed vectors with the values and used them in the statistical classifier based on discriminant analysis. The results of class classification for irises, ocular prostheses and colored contact lenses are shown in Table V. The

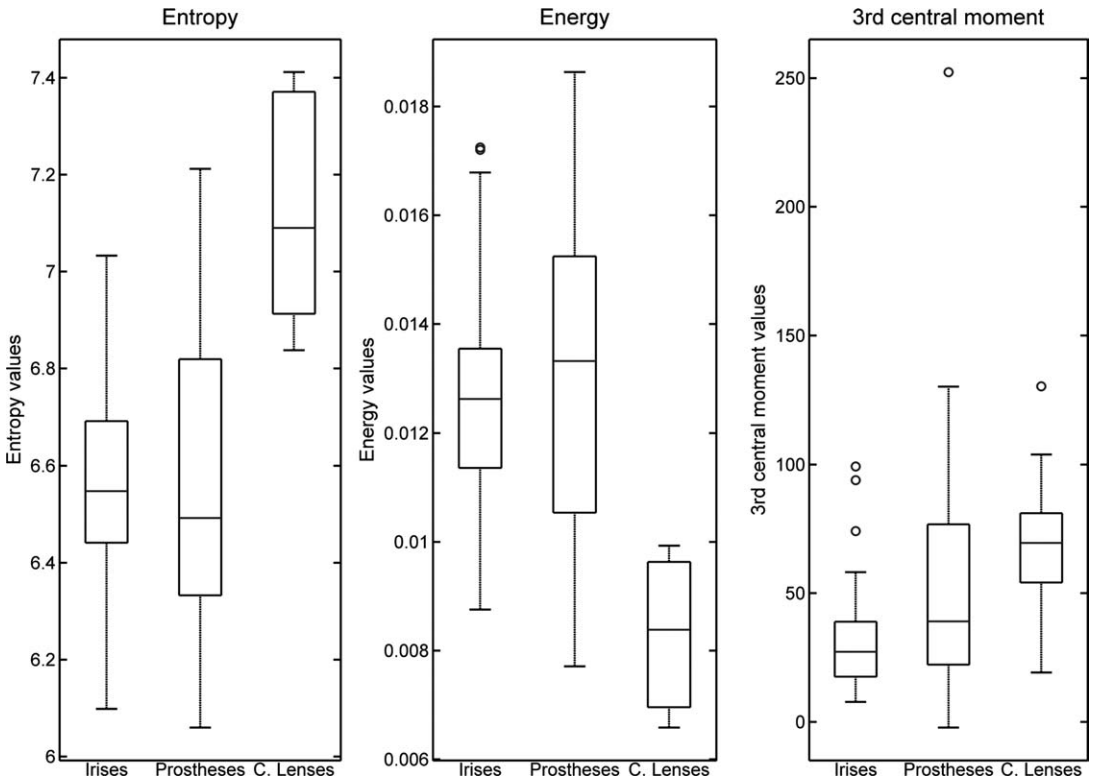

FIG. 9. First order statistical descriptors for texture analysis: entropy, energy and 3rd central moment.

TABLE V. Results in class classification via linear discriminant analysis using first and second order statistical features for texture description.

	Percentage of correct class classification (%)		
Statistics	Irises	Prostheses	C. Lenses
First order	68.4	43.3	64.7
Second order	88.4	82.1	100.0

percentages of this table show the ratio of samples that being a member of one of the three classes were classified by the algorithm effectively as belonging to its correspondent class by just attending to its textural features. Although, for the first order statistics some of the samples could be properly classified, meaning that they were related to different inherent textures, these percentages were still not very high.

Figure 10 shows the distribution of some of the textural descriptors extracted from the co-occurrence matrices. The second order statistical descriptors corresponding to the subject with dark brown irises who participated in the measurement of all the contact lenses were of $Ep = 8.54$, $En = 0.35 \times \cdot 10^{-3}$, and $C = 215.2$.

The use of second order descriptors led to more conclusive results in terms of percentages of proper or correct identification of samples (Table V) and provided percentages of correct class classification of over 80% in all sample sets. Specifically, a 100% rate was found for the group of contact lenses. This means that real irises, ocular prostheses and colored contact lenses are related to different textures, to the point that it is possible to distinguish them by the features used.

CONCLUSIONS

In this study, we analyzed the color and texture of 106 real irises, 68 ocular prostheses, and 17 colored contact lenses. A high resolution image of the samples was obtained by means of a multispectral system, and the CIE *L*a*b** color coordinates were computed pixel by pixel under the illuminant D65 and the CIE-1931 standard observer. An automatic algorithm was developed to classify the samples into three color groups (brown, blue, and green), which enabled us to perform a deeper analysis of the iris color reproduction.

We compared the color of the samples by studying color gamuts in the CIE *L*a*b** color space and their overlapping zones. Moreover, the CIEDE2000 color difference formula was also used to look for the ocular prosthesis and contact lens that were closest to each human iris. The results suggest that the colors of ocular prostheses are similar to those of real irises with respect to mean colorimetric values, with percentages of superposition of the color gamuts of around 80% and minimum CIEDE2000 color differences that are similar to or below 2.5. However, in the case of colored contact lenses, larger color deviations were found, mainly in the blue and green color groups. This may be due to the dark iris used in the contact lenses measurements and the limited number of lenses analyzed. Furthermore, it must be taken into account that colors of colored contact lenses are more of-

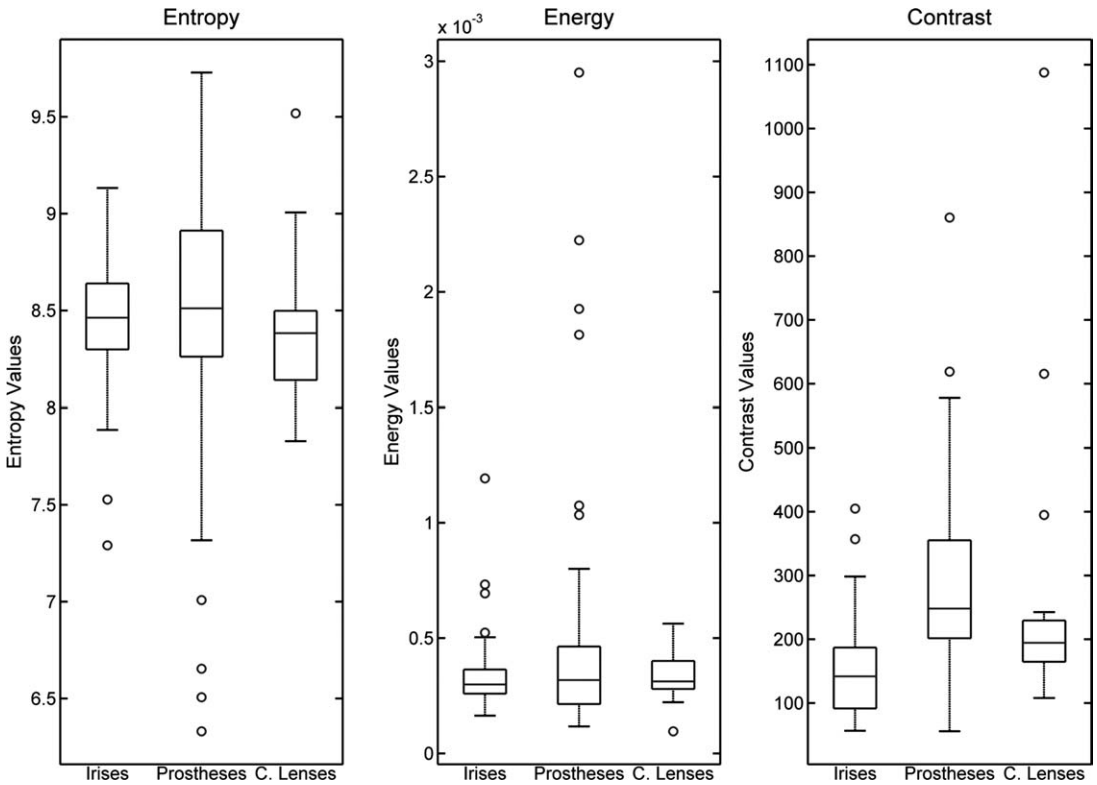

FIG. 10. Second order statistical descriptors for texture analysis: entropy, energy, and contrast.

ten related to fashion trends than color reproduction. Conclusions reached when performing the same analysis of color among samples but under the illuminant A were almost identical to those found with the D65 illuminant.

Finally, we performed an analysis of the color distribution over the entire iris surface using the pixelwise information acquired through the multispectral system. The analysis of first order statistics was not enough to establish that the irises, ocular prostheses and colored contact lenses had a clearly different texture. However, it did show that there was a tendency to different textures, which was subsequently confirmed by the results provided by second order statistical analyses and the assessments of class identification. The rates of correct classification were over 80% for all the samples (100% in the case of colored contact lenses), which suggests that clear textural differences exist amongst samples.

The results of this study can help to establish a strategy for improving the industrial reproduction of the color and spatial structure of ocular prostheses and colored contact lenses, to make them more similar to real irises. Future work is oriented to analyze the spectral data of the samples, which can be useful to study specific differences in the properties of the materials used in the manufacturing process.

ACKNOWLEDGMENTS

Jorge Herrera is grateful for the support of the Commission for Universities and Research of the Catalan Government's, Department of Innovation, Universities and Enterprise and to the European Social Fund.

1. Imesch PD, Wallow IHL, Albert DM. The color of the human eye: A review of morphologic correlates and of some conditions that affect iridial pigmentation. Surv Ophthalmol 1997;41:S117–S123.
2. German EJ, Hurst MA, Wood D, Gilchrist J. A novel system for the objective classification of iris colour and its correlation with response to 1% tropicamide. Ophthalmic Physiol Opt 1998;18:103–110.
3. Sturm RA, Frudakis TN. Eye colour: Portals into pigmentation genes and ancestry. Trends Genet 2004;20:327–332.
4. Daugman JG. High confidence visual recognition of persons by a test of statistical independence. IEEE Trans Pattern Anal Mach Intell 1993;15:1148–1161.
5. Wildes RP. Iris recognition: An emerging biometric technology. Proc IEEE 1997;85:1348–1363.
6. Ma L, Tan T, Wang Y, Zhang D. Personal identification based on iris texture analysis. IEEE Trans Pattern Anal Mach Intell 2003;25:1519–1533.
7. Budde WE, Velten IM, Jonas JB. Optics disc size and iris color. Arch Ophthalmol 1998;116:545.
8. Seddon J, Sahagian C, Glynn R, Sperduto R, Gragoudas E. Evaluation of an iris color classification system. The eye disorders case-control study group. Invest Ophthalmol Vis Sci 1990;31:1592–1598.
9. Hammond Jr BR, Fuld K, Snodderly MD. Iris color and macular pigment optical density. Exp Eye Res 1996;62:293–298.
10. Melgosa M, Rivas MJ, Mez LG, Hita E. Towards a colorimetric characterization of the human iris. Ophthalmic Physiol Opt 2000;20:252–260.
11. Boyce C, Ross A, Monaco M, Hornak L, Li X. Multispectral iris analysis: A preliminary study. IEEE 2006;1:51–59.
12. Takamoto T, Schwartz B, Cantor LB, Hoop JS, Steffens T. Measurement of iris color using computerized image analysis. Curr Eye Res 2001;22:412–419.
13. Fan S, Dyer C, Hubbard L. Quantification and Correction of Iris Color. Madison: University of Wisconsin; 2003. Technical Report 1495. 10 p.
14. Nabti M, Bouridane A. An effective and fast iris recognition system based on a combined multiscale feature extraction technique. Pattern Recognit 2008;41:868–879.
15. Zhuoshi W, Xianchao Q, Zhenan S, Tieniu T. Counterfeit iris detection based on texture analysis. Int Conf Pattern Recognit 2008;1:1–4.
16. Bowyer KW, Hollingsworth K, Flynn PJ. Image understanding for iris biometrics: A survey. Comput Vis Image Underst 2008;110:281–307.
17. de Oliveira PR, Walline JJ. Cosmetic and prosthetic contact lenses. In: Mannis MJ, Zadnik K, Coral-Ghanem C, Kara-José N, editors. Contact lenses in ophthalmic practice. New York: Springer-Verlag; 2004. p 191–197.
18. Port MJA. Cosmetic and prosthetic lenses. In: Phillips AJ, Stone J, editors. Contact lenses, 3rd ed. Boston: Butterworth-Heineman; 1989. p 789–796.
19. Lefohn A, Caruso R, Reinhard E, Budge B. An ocularist's approach to human iris synthesis. IEEE Comput Graph Appl 2003;23:70–75.
20. Francois G, Gautron P, Breton G, Bouatouch D. Image-based modeling of the human eye. IEEE Trans Vis Comput Graph 2009;15:815–827.
21. Imai FH. Preliminary experiment for spectral reflectance estimation of human iris using a digital camera. New York: Munsell Lab Report; 2002. 28 p.
22. de Lasarte M. Thorough characterization and analysis of a multispectral imaging system developed for color measurement. Ph.D thesis. Terrassa: Technical University of Catalonia; 2009. 352 p.
23. Vilaseca M, Mercadal R, Pujol J, Arjona M, de-Lasarte M, Huertas R, Melgosa M, Imai FH. Characterization of the human iris spectral reflectance with a multispectral imaging system. Appl Opt 2008;47:5622–5630.
24. de Lasarte M, Pujol J, Arjona M, Vilaseca M. Optimized algorithm for the spatial nonuniformity correction of an imaging system based on a charge-coupled device color camera. Appl Opt 2007;46:167–174.
25. Vilaseca M, Pujol J, Arjona M. Illuminant influence on the reconstruction of near-infrared spectra. J Imaging Sci Technol 2004; 48:111–119.
26. Vilaseca M, Pujol J, Arjona M, de Lasarte M. Multispectral system for reflectance reconstruction in the near-infrared region. Appl Opt 2006;45:4241–4253.
27. CIE 142–2001. Improvement to industrial colour-difference evaluation. ISBN: 9783901906084.
28. Gonzalez RC, Woods RE, Eddins SL. Digital image processing using MATLAB. Upper Saddle River, NJ: Prentice Hall; 2004. 620 p.
29. Ritter GX, Wilson JN. Handbook of computer vision algorithms in image algebra. Boca Ratón: CRC Press; 2001. 425 p.
30. Haralick RM, Shanmugam K, Dinstein IH. Textural features for image classification. IEEE Trans Syst Man Cybern 1973;3:610–621.
31. Materka A, Strzelecki M. Texture analysis methods—A review. Report no: COST B11. Brussels: Technical University of Lodz; 1998. 33 p.
32. Julesz B, Gilbert EN, Shepp LA, Frisch HL. Inability of humans to discriminate between visual textures that agree in second-order statistics—Revisited. Perception 1973;2:391–405.
33. Landy MS, Graham N. Visual perception of texture. In: Chalupa LM, Werner JS, editors. The visual neurosciences. Cambridge: MIT Press; 2004. p 1106–1118.
34. Rencher AC. Methods of multivariate analysis. New York: John Wiley and Sons; 2002. 732 p.
35. Williamson DF, Parker RA, Kendrick JS. The box plot: A simple visual method to interpret data. Ann Intern Med 1989;110:916–921.
36. Barber CB, Dobkin DP, Huhdanpaa H. The quickhull algorithm for convex hulls. ACM Trans Math Softw 1996;22:469–483.